Regenerative Therapy 24 (2023) 582–591

Contents lists available at ScienceDirect

Regenerative Therapy

journal homepage: http://www.elsevier.com/locate/reth

Original Article

Early revascularization activates quiescent dental pulp stem cells following tooth replantation in mice

Hiroto Sano [a], Kuniko Nakakura-Ohshima [b], Angela Quispe-Salcedo [c], Yasuo Okada [a], Takuichi Sato [d], Hayato Ohshima [c, *]

[a] Department of Pathology, The Nippon Dental University School of Life Dentistry at Niigata, Niigata, Japan
[b] Division of Pediatric Dentistry, Department of Oral Health Science, Niigata University Graduate School of Medical and Dental Sciences, Niigata, Japan
[c] Division of Anatomy and Cell Biology of the Hard Tissue, Department of Tissue Regeneration and Reconstruction, Niigata University Graduate School of Medical and Dental Sciences, Niigata, Japan
[d] Division of Clinical Chemistry, Department of Medical Technology, Niigata University Graduate School of Health Sciences, Niigata, Japan

ARTICLE INFO

Article history:
Received 1 August 2023
Received in revised form
17 October 2023
Accepted 26 October 2023

Keywords:
Dental pulp
Mice
Tooth replantation
Revascularization
Odontoblast

ABSTRACT

Introduction: The intentional perforation of the pulp chamber floor before tooth replantation promotes pulpal healing by facilitating the revascularization of the pulp cavity. This study aimed to elucidate the effects of this method on the dynamics of quiescent dental pulp stem cells (DPSCs).
Methods: The right and left maxillary first molars of Crlj:CD1 mice and TetOP-histone 2B (H2B)-green fluorescent protein (GFP) mice were extracted. The left molars were immediately replanted as the control group (CG), whereas the pulp chamber floor of the right molars were perforated before the tooth was replanted as the experimental group (EG). Immunohistochemistry for Nestin and GFP, and quantitative RT-PCR for *Nestin*, *Opn*, *CD11c*, and *Oct3/4* mRNA were performed.
Results: The rate of Nestin-positive perimeter along the pulp–dentin border in the EG tended to be higher than that of the CG at days 5 and 7 and was significantly increased between days 3 and 7. The rate of GFP-positive cells in the EG was significantly higher than that of the CG at days 5 and/or 7 in the mesial and middle coronal pulp. *CD11c* mRNA in the EG at day 5 was significantly higher than that of the CG and tended to be higher than that of the CG during the observation period. *Oct3/4* mRNA expression in the EG was significantly higher than that of the CG at day 7.
Conclusions: The current experimental model demonstrated the promotion of the survival of DPSCs and their differentiation into odontoblast-like cells (OBLCs). Thus, the use of this model is expected to clarify the crosstalk mechanism between immune cells, including macrophages and dendritic cells, and DPSCs with regards to pulpal healing after tooth replantation. It also provides insight into the differentiation process of DPSCs into OBLCs.

1. Introduction

Tooth avulsion is one of the most serious dental traumas, where the tooth is completely dislocated from the alveolar socket and results in the ablation of the blood vessels and nerves at the apical foramina [1,2]. Tooth replantation is the first choice of the treatment for tooth avulsion [3]. In addition to providing nutrition and sensation, dental pulp has a high regenerative capability to recover after tooth injury. The condition of the avulsed tooth prior to replantation, state of the alveolar bone, and degree of root formation, especially the size of the apical foramina, are critical factors that influence pulpal healing after tooth replantation [4]. Securing the routes from the periodontal tissue to the dental pulp for early revascularization is also essential for the pulpal healing after tooth replantation [5]. Experimental animal models of tooth replantation have shown that pulpal healing occurs after extensive damage and the degeneration of odontoblasts in the pulp cavity after the injury.

Abbreviations: EG, experimental group; CG, control group; H&E, hematoxylin and eosin; GFP, green fluorescent protein; H2B, histone 2B; ICR, institute of cancer research; DPSCs, dental pulp stem cells; OBLCs, odontoblast-like cells; SCAP, stem cells from the apical papilla; OPN, osteopontin.

* Corresponding author.
E-mail address: histoman@dent.niigata-u.ac.jp (H. Ohshima).

Peer review under responsibility of the Japanese Society for Regenerative Medicine.

https://doi.org/10.1016/j.reth.2023.10.004

At least two patterns of pulpal healing have been demonstrated to occur; namely tertiary dentin formation and bone tissue formation [6,7]. Since root resorption and ankylosis are readily induced when the pulp cavity is replaced with bone tissue [8], the occurrence of tertiary dentin formation in the pulp cavity after tooth replantation is important for a better prognosis after tooth replantation. Furthermore, the appearance of dendritic cells at the pulp–dentin border after tooth replantation triggers the differentiation of odontoblast-like cells (OBLCs), while the appearance of osteoclast-lineage cells in the pulp cavity leads to the differentiation of osteoblasts [9]. Therefore, the migration of dendritic cells to the pulp cavity is vital to induce dentin formation after tooth replantation.

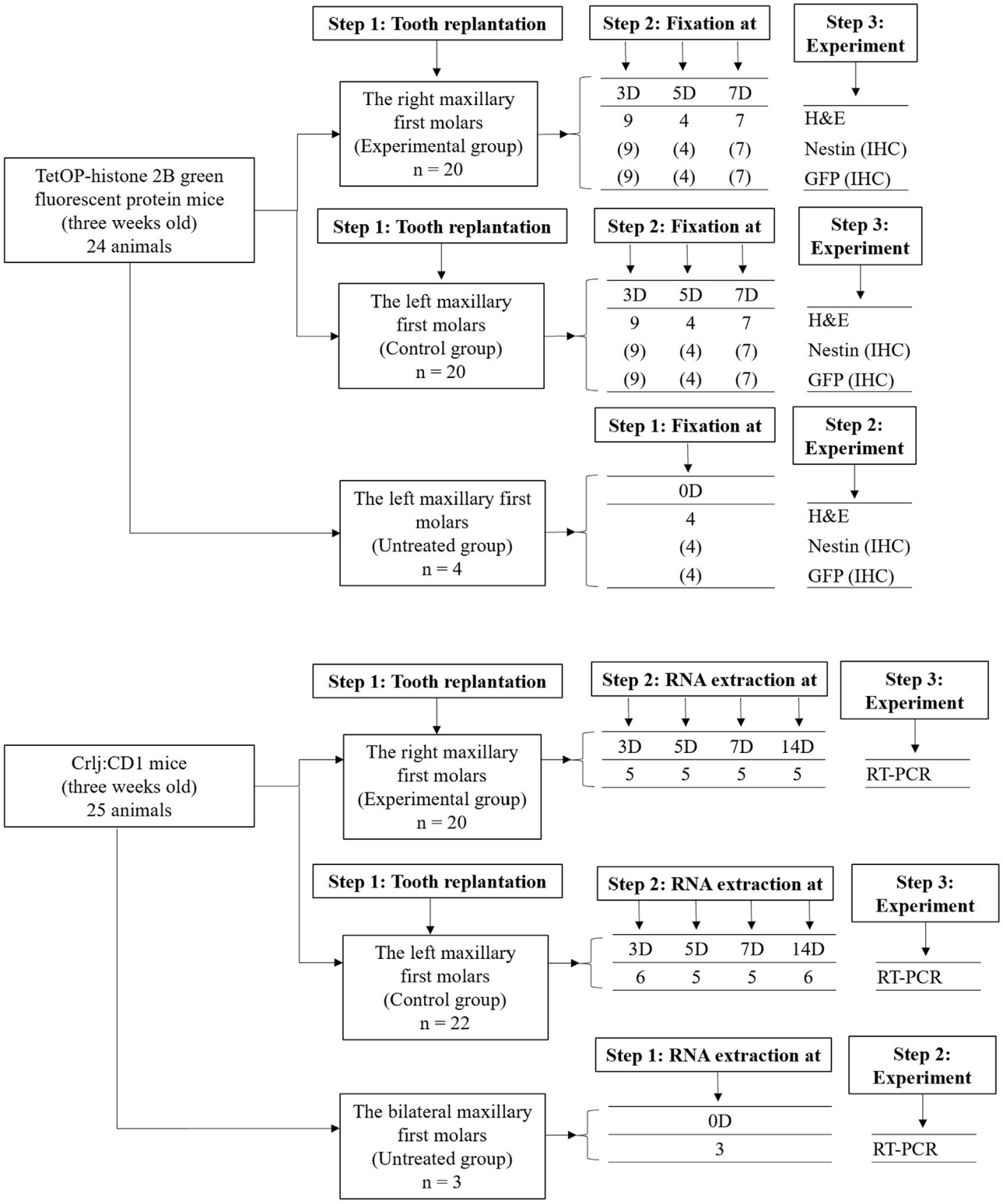

Fig. 1. Number of animals used and schedule for each experiment.

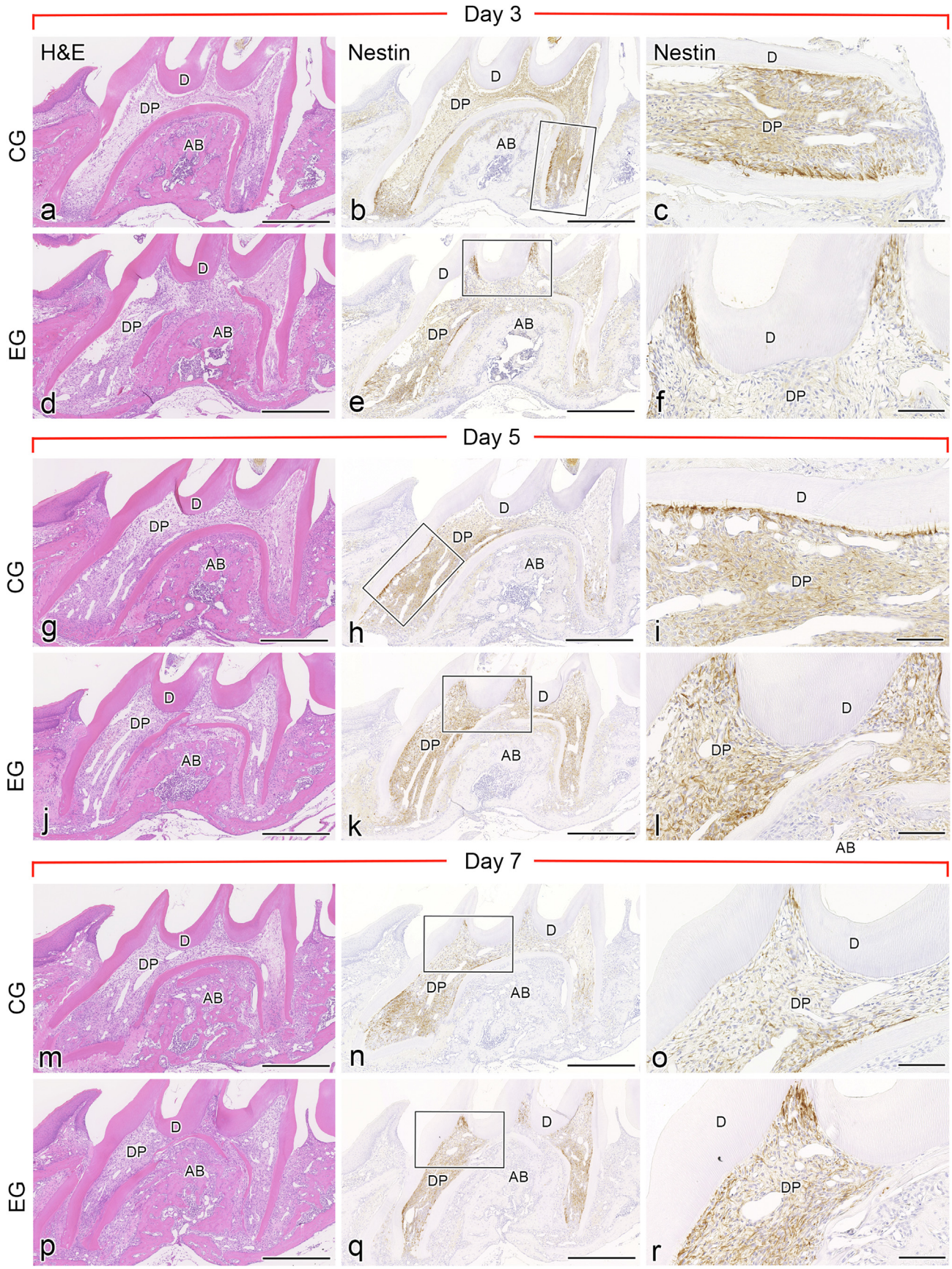

Fig. 2. Hematoxylin and eosin stained (a, d, g, j, m, p) and Nestin immunohistochemically stained sections (b, c, e, f, h, i, k, l, n, o, q, r) of the replanted teeth in the control group (CG) (a–c, g–i, m–o) and experimental group (EG) (d–f, j–l, p–r) 3 (a–f), 5 (g–l), and 7 days (m–r) after tooth replantation. The images c, f, i, l, o, and r are higher magnification views of

During the pulpal healing process after tooth injury, adult stem cells in the pulp cavity become the source of the cells for dental pulp reconstruction. Adult stem cells include active stem cells that are in the cell cycle and quiescent stem cells that are out of the cell cycle and have low metabolic activity [10]. Dental pulp stem cells (DPSCs) are considered to be quiescent stem cells that rarely self-renew under normal conditions but actively divide after tooth injury [11]. Experimental animal models of tooth injury have revealed that DPSCs are localized in various niches. DPSCs are present around the blood vessels in the central pulp tissue, and the progenitor cells that have the capability to differentiate into OBLCs after tooth injury are located in the subodontblastic layer [12]. Stem cells from the apical papilla (SCAP), which also have the ability to differentiate into OBLCs, are also present in the apical papilla [13,14], suggesting their involvement in pulpal healing after tooth injury. The disappearance of quiescent DPSCs from the dental pulp after tooth replantation triggers the formation of bone tissue [15]. Therefore, the maintenance of quiescent DPSCs that are capable of differentiating into OBLCs after tooth replantation is essential to induce tertiary dentin formation in the pulp cavity of replanted teeth [11]. In an experimental animal model of tooth replantation, intentional root resection before tooth replantation promoted the early revascularization of the pulp cavity which resulted in tertiary dentin formation [16]. In the case of human teeth, an apicoectomy before the autogenic transplantation of mature teeth induced revascularization [17]. Although root resection induces the early revascularization of the coronal pulp by shortening the root length and alleviates the deterioration of the pulpal healing due to occlusal trauma after surgery, root resection results in the loss of the SCAP.

The intentional perforation of the floor of the pulp chamber before tooth replantation is a method that promotes pulpal healing by facilitating the revascularization of the pulp cavity as well as maintaining the root length and SCAP [5]. This method is expected to be clinically applied to tooth replantation and the autogenic transplantation of teeth with mature or immature roots. In replanted teeth with the intentional perforation of the pulp chamber floor, early revascularization occurs via the perforation site, which promotes tertiary dentin formation and suppresses bone tissue formation in the pulp cavity due to the higher cell proliferative activity and fewer apoptotic cells compared with the immediately replanted teeth without pulp chamber floor perforation. Therefore, the intentional pulp chamber floor perforation before tooth replantation is presumed to affect the dynamics of the quiescent DPSCs. However, the effect of this method on the dynamics of the quiescent DPSCs remains unclear. The key question of this study is how the intentional pulp chamber floor perforation before tooth replantation affects the survival and activation of quiescent DPSCs.

An experimental technique has been established using TetOP-histone 2B (H2B)-green fluorescent protein (GFP) mice, in which all cells are labeled with GFP by doxycycline administration during the prenatal stage, to chase the GFP label that are diluted by cell division [18–20]. Studies using this technique have demonstrated that the label-retaining cells in the dental pulp are expected to be quiescent DPSCs that seldom divide. This study aimed to clarify the effects of the intentional pulp chamber floor perforation on the dynamics of quiescent DPSCs using the prenatal labeling technique to label quiescent DPSCs in TetOP-H2B-GFP mice. In addition, immunohistochemistry was used to test for Nestin, which is an odontoblasts and OBLCs marker, and quantitative RT-PCR was performed to measure the levels of *Nestin*, *Osteopontin (Opn)*, and *CD11c*, which is a marker of dendritic cells, and *Oct3/4*, which is a stem cell marker.

2. Methods

2.1. Animals

All animal experiments were conducted in strict accordance with the ARRIVE guidelines [21] and the protocol was reviewed by the Institutional Animal Care and Use Committee and approved by the President of Niigata University (Approval number: SA00784). Male and female TetOP-H2B-GFP mice (three weeks old) were used for the immunohistochemical analysis of Nestin and GFP. For the GFP transgene expression, doxycycline (2 mg/mL, supplemented with 50 mg/mL sucrose) was added to the drinking water at embryonic days 16.5 or 17.5 and supplied for two days. Male Crlj:CD1 Institute of Cancer Research (ICR) mice (three weeks old) (Charles River Laboratories Japan, Yokohama, Japan) were used for quantitative RT-PCR analysis. The animals were housed in a specific pathogen-free and temperature-controlled environment with unrestricted access to food and water.

2.2. Tooth replantation

Tooth replantation was performed as described in a previous study [5]. Briefly, both the right and left maxillary first molars of the TetOP-H2B-GFP and ICR mice were extracted. The left molars were immediately replanted as the control group (CG), whereas the pulp chamber floor of the right molars was perforated with a tungsten carbide bur (diameter = 0.5 mm) before tooth replantation as the experimental group (EG).

2.3. Tissue preparation

Forty-nine animals were used for the collection of materials (Fig. 1). The animals were deeply anesthetized with a mixed solution of Domitor® (Nippon Zenyaku Kogyo Co, Ltd, Koriyama, Japan), midazolam (Sandoz KK, Tokyo, Japan), Vetorphale® (Meiji Seika Pharma Co, Ltd, Tokyo, Japan) [5], and physiological saline, and then perfused with a 4 % paraformaldehyde solution in a 0.1 M phosphate buffer (pH 7.4). After decalcification in a 10 % EDTA-2Na solution, the specimens were dehydrated, embedded in paraffin, and sectioned into 4-μm thick sagittal slices. The sections were subjected to hematoxylin and eosin staining and immunohistochemistry.

2.4. Immunohistochemical and immunofluorescent procedures

For the immunohistochemical staining, sample sections were processed according to the EnVision system (Dako Japan, Tokyo, Japan), and the primary antibodies used in this study were anti-Nestin (mouse monoclonal, #MAB353, EMD Millipore, Billerica,

the boxed areas in images b, e, h, k, n, and q, respectively. (a–f) Preexisting odontoblasts in the pulp cavity of both the CG and EG are extensively degenerated and lost most of their Nestin-positive immunoreactivity. (b, c) In the CG, Nestin-positive cells are not observed in the coronal pulp, and Nestin-positive cells align only in some parts of the roots. (e, f) Nestin-positive cells are observed in the pulp horns and near the perforation site. (g, h) Revascularization of the coronal pulp are not completed. (i) Revascularization occurs in the root pulps where Nestin-positive cells align. (j–l) Revascularization is extended throughout the pulp cavity via both the apical foramina and perforation site, and Nestin-positive filamentous structures are extensively observed throughout the pulp cavity including near the pulp horns as well as the occurrence of Nestin-positive odontoblasts or odontoblast-like cells (OBLCs). (m–o) The alignment of Nestin-positive OBLCs expands into the coronal pulp with revascularization progression, while the Nestin-positive reactivity near the pulp horns is limited. (p–r) Revascularization in the pulp cavity is nearly complete, and the Nestin-positive odontoblasts or OBLCs are observed along the pulp-dentin border in the entire pulp, including the pulp horns. D, dentin; DP, dental pulp; AB, alveolar bone. Scale bars = (a, b, d, e, g, h, j, k, m, n, p, q) 500 μm, (c, f, i, l, o, r) 100 μm.

MA, USA; diluted to 1:500) and anti-GFP (rabbit polyclonal, #598, Medical & Biological Laboratories Co., Nagoya, Japan; diluted to 1:1000). For the fluorescent immunohistochemistry, sections were incubated with an anti-Nestin antibody followed by a biotinylated anti-mouse IgG (horse polyclonal, #BA2001, Vector Laboratories, Burlingame, CA, USA; diluted to 1:100) and Texas red-conjugated streptavidin. Cell nuclei were counterstained with 4',6-diamidino-2-phenylindole (DAPI; VECTASHIELD Mounting Medium with DAPI, Vector Laboratories). Fluorescent images were deconvoluted with imaging software (NIS-Elements Ver 5.30: Nikon Solutions Co, Ltd, Tokyo, Japan).

2.5. Quantitative RT-PCR

Quantiative RT-PCR was performed to quantify *Nestin*, *Opn*, *CD11c*, and *Oct3/4* mRNA relative to *β-actin* mRNA. Total RNA was extracted from the dental pulp of extracted maxillary first molars of the ICR mice using the TRIzol system (Invitrogen, Carlsbad, CA, USA). The cDNA was synthesized using the Prime Script 1st strand cDNA Synthesis Kit (Takara, Otsu, Japan), and quantitative real-time PCR was performed using SYBR1 Premix Ex Taq II (Takara). Amplification was performed using the Thermal Cycler Dice (Takara), and the PCR protocol consisted of initial heat activation at 95 °C for 30 s, followed by 50 cycles of 95 °C for 5 s and 60 °C for 30 s, and dissociation was performed at 95 °C for 15 s and 60 °C for 30 s. The relative gene expression levels were calculated relative to the levels of *β-actin* mRNA using the comparative Ct (2−ΔΔCt) method. The primers used for amplification were forward (5′-GAC CAG GTG CTT GAG AGA CT-3′) and reverse (5′-ACC TGG TCC TCT GCT TCT TC-3′) for *Nestin*, forward (5′-TTT ACA GCC TGC ACC C-3′) and reverse (5′-CTA GCA GTG ACG GTC T-3′) for *Opn*, forward (5′-ACA CAG TGT GCT CCA GTA TGA-3′) and reverse (5′-GCC CAG GGA TAT GTT GAC AGC-3′) for *CD11c*, forward (5′- TCT TTC CAC CAG GCC CCC GGC TC -3′) and reverse (5′-TGC GGG CGG ACA TGG GGA GAT CC -3′) for *Oct3/4*, and forward (5′-GTG GGA ATG GGT CAG AAG GA-3′) and reverse (5′-CTT CTC CAT GTC GTC CCA GT-3′) for *β*-actin.

2.6. Statistical analysis

The rate of Nestin-positive perimeter on the pulp–dentin border in the mesial and distal pulps of the sections that were immunohistochemically stained for Nestin was measured using Image J software (Image J 1.53k, NIH). The rate of GFP-positive cells in the images was determined using a computerized image analysis system, Patholoscope ver.1.2.1 (Mitani Corp.). The rate of Nestin-positive perimeter and GFP-positive cells and mRNA expression of *Nestin*, *Opn*, *CD11c*, and *Oct3/4* at each time point following tooth replantation were compared using one-way analysis of variance (ANOVA) after confirming data normality and homogeneity of variance, followed by the Bonferroni test for multiple comparisons. Comparisons between the data from the control group and the experimental group were conducted using the Student's *t*-test with statistical software (SPSS 16.0 J for Windows; SPSS Japan, Tokyo, Japan). The samples showing no normal distribution were compared by Kruskal–Wallis test for more than three groups or Mann–Whitney *U*-test for two groups [5].

3. Results

3.1. Chronological changes of Nestin expression in the dental pulp following tooth replantation

In the untreated teeth, Nestin expression was observed in the odontoblasts that aligned along the pulp–dentin border (Supplementary Fig. 1). At day 3, odontoblasts in the pulp cavity of both the CG and EG were extensively degenerated and lost most of their Nestin-positive immunoreactivity (Fig. 2a–f). In the CG, Nestin-positive cells were not observed in the coronal pulp and were only aligned in some parts of the roots (Fig. 2b and c). In the EG, the Nestin-positive cells aligned in the pulp horns and near the perforation site (Fig. 2e and f). At day 5, the revascularization in the coronal pulp was not completed in the CG (Fig. 2g and h), whereas revascularization occurred in the root pulps where Nestin-positive cells were aligned (Fig. 2i). In the EG, revascularization extended throughout the pulp cavity via both the apical foramina and perforation site. In addition, Nestin-positive filamentous structures were extensively observed in the entire pulp cavity including near the pulp horns as well as the occurrence of Nestin-positive odontoblasts or OBLCs (Fig. 2k and l). At day 7, the alignment of Nestin-positive OBLCs expanded into the coronal pulp according to the revascularization progression in the CG, while Nestin-positive reactivity near the pulp horns was limited (Fig. 2m–o). In the EG, revascularization in the pulp cavity was nearly complete, and the Nestin-positive odontoblasts or OBLCs were observed to align along the pulp–dentin border in the entire pulp, including the pulp horns (Fig. 2p–r). The rate of Nestin-positive perimeter in the EG tended to be higher than that of the CG at days 5 and 7 in both the mesial

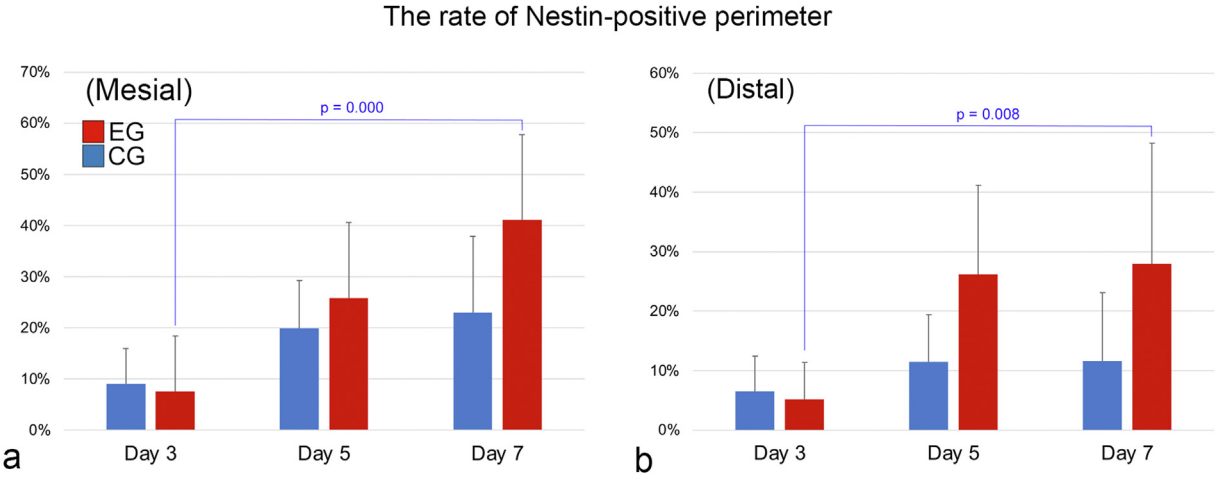

Fig. 3. The rates of Nestin-positive perimeter in the mesial (a) and distal pulps (b) during days 3–7. (a, b) The rate of Nestin-positive perimeter in the experimental group (EG) tends to be higher than that of the control group (CG) at days 5 and 7 in both the mesial and distal pulps and significantly increases between days 3 and 7 in both the mesial and distal pulps. The rate of Nestin-positive perimeter in the distal pulp at day 7 tends to be lower than that of the mesial pulp in both the CG and EG.

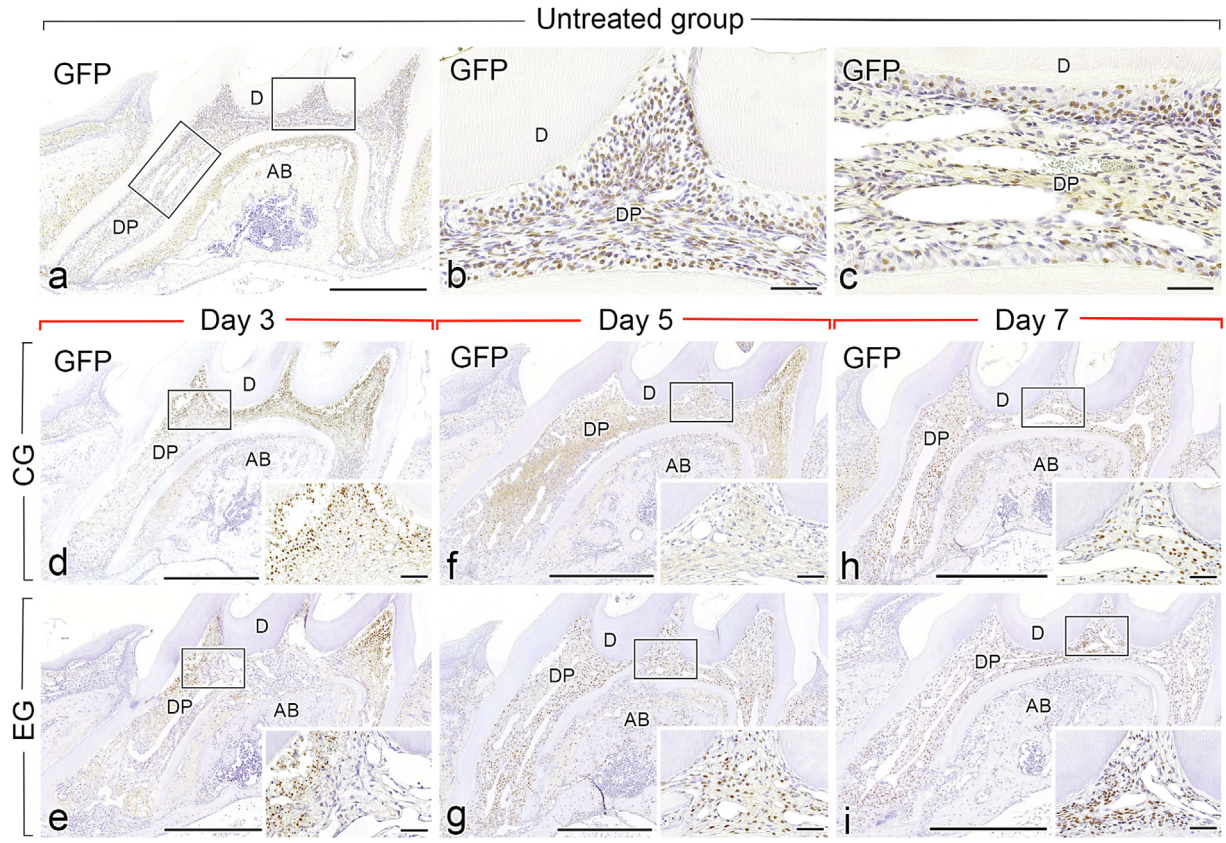

Fig. 4. Green fluorescent protein (GFP) immunohistochemical sections of the untreated teeth (a–c) and replanted teeth in the control group (CG) (d, f, h) and experimental group (EG) (e, g, i) 3 (d, e), 5 (f, g), and 7 days (h, i) after tooth replantation. The insets are higher magnification views of the boxed areas. (a–c) GFP-positive cells are observed throughout the pulp cavity. (b) Dense GFP-positive cells are observed in the odontoblast and subodontoblastic layers, and central pulp tissue of the coronal pulp. (c) The number of GFP-positive cells in the root pulps is fewer than that in the coronal pulp and the cells are predominantly located in the odontoblast layer and central pulp tissue. (d) The GFP-positive cells are localized in the coronal pulp. (e) The GFP-positive cells are observed in the coronal pulp except near the perforation site. (f) The CG exhibit a notable decrease in the number of GFP-positive cells at day 5 compared with that at day 3. (g) The GFP-positive cells are distributed throughout the pulp cavity at day 5 in the EG. (h, i) The GFP-positive cells are arranged throughout the pulp cavity in both the CG and EG. D, dentin; DP, dental pulp; AB, alveolar bone. Scale bars = (a, d–i) 500 μm, (b, c, and insets) 50 μm.

and distal pulps and significantly increased between days 3 and 7 in both the mesial and distal pulps (Fig. 3a and b). The rate of Nestin-positive perimeter in the distal pulp at day 7 tended to be lower than in the mesial pulp in both the CG and EG (Fig. 3a and b).

3.2. Dynamics of GFP-positive cells following tooth replantation

GFP-positive cells were observed throughout the pulp cavity in the untreated group (Fig. 4a–c). Dense GFP-positive cells were observed in the odontoblast and subodontoblastic layers, and central pulp tissue of the coronal pulp (Fig. 4b). The number of GFP-positive cells in the root pulps was smaller compared with the number in the coronal pulp and the cells were predominantly located in the odontoblast layer and central pulp tissue (Fig. 4c). At day 3, the GFP-positive cells were localized in the coronal pulp in the CG (Fig. 4d), whereas they were observed in the coronal pulp, except near the perforation site, in the EG (Fig. 4e). The CG exhibited a notable decrease in the number of GFP-positive cells at day 5 compared with that at day 3 (Fig. 4f). In contrast, the GFP-positive cells were distributed throughout the pulp cavity at day 5 in the EG (Fig. 4g). At day 7, the GFP-positive cells were arranged throughout the pulp cavity in both the CG and EG (Fig. 4h and i). The rate of GFP-positive cells in the EG tended to be lower than that of the CG in the mesial and middle coronal pulps at day 3, whereas the rate of GFP-positive cells in the EG was significantly higher than that of the CG at day 5 in the mesial coronal pulp and at days 5 and 7 in the middle coronal pulp (Fig. 5a, c). In the distal coronal pulp, the rate of GFP-positive cells at days 5 and 7 was significantly lower than that on day 3 in both the CG and EG (Fig. 5b). The rate of GFP-positive cells in the roots progressively increased over time in both the CG and EG, reaching the same or higher rate of GFP-positive cells than the untreated group at day 7 (Fig. 5d–g). In the EG, the rate of GFP-positive cells in the roots tended to be higher than that of the CG, and the rate of GFP-positive cells in the mesial upper root in the EG was significantly higher than that of the CG at day 7 (Fig. 5d). In the lower roots, the rate of GFP-positive cells at day 7 was significantly increased compared with that at day 3 in both the CG and EG except for the mesial lower root of the CG (Fig. 5f and g). GFP-positive cells that were aligned along the pulp–dentin border showed Nestin-immunoreactivity at day 7 in both the CG and EG (Fig. 6).

3.3. Quantitative RT-PCR analysis of pulpal healing-related factors

Quantitative RT-PCR was performed to quantify *Nestin*, *Opn*, *CD11c*, and *Oct3/4* mRNA relative to *β-actin* mRNA. *Nestin* mRNA in both the CG and EG was significantly decreased at days 3, 5, 7, and 14 compared with that of the untreated teeth ($p < 0.001$ between each group) (Fig. 7a). *Opn* mRNA expression in the EG tended to be lower than that of the CG at day 3 and to be higher than that of the CG at day 14 (Fig. 7b). *CD11c* mRNA was decreased at the day 3 in both the CG and EG and increased at day 5 in the EG, and at day 7 in

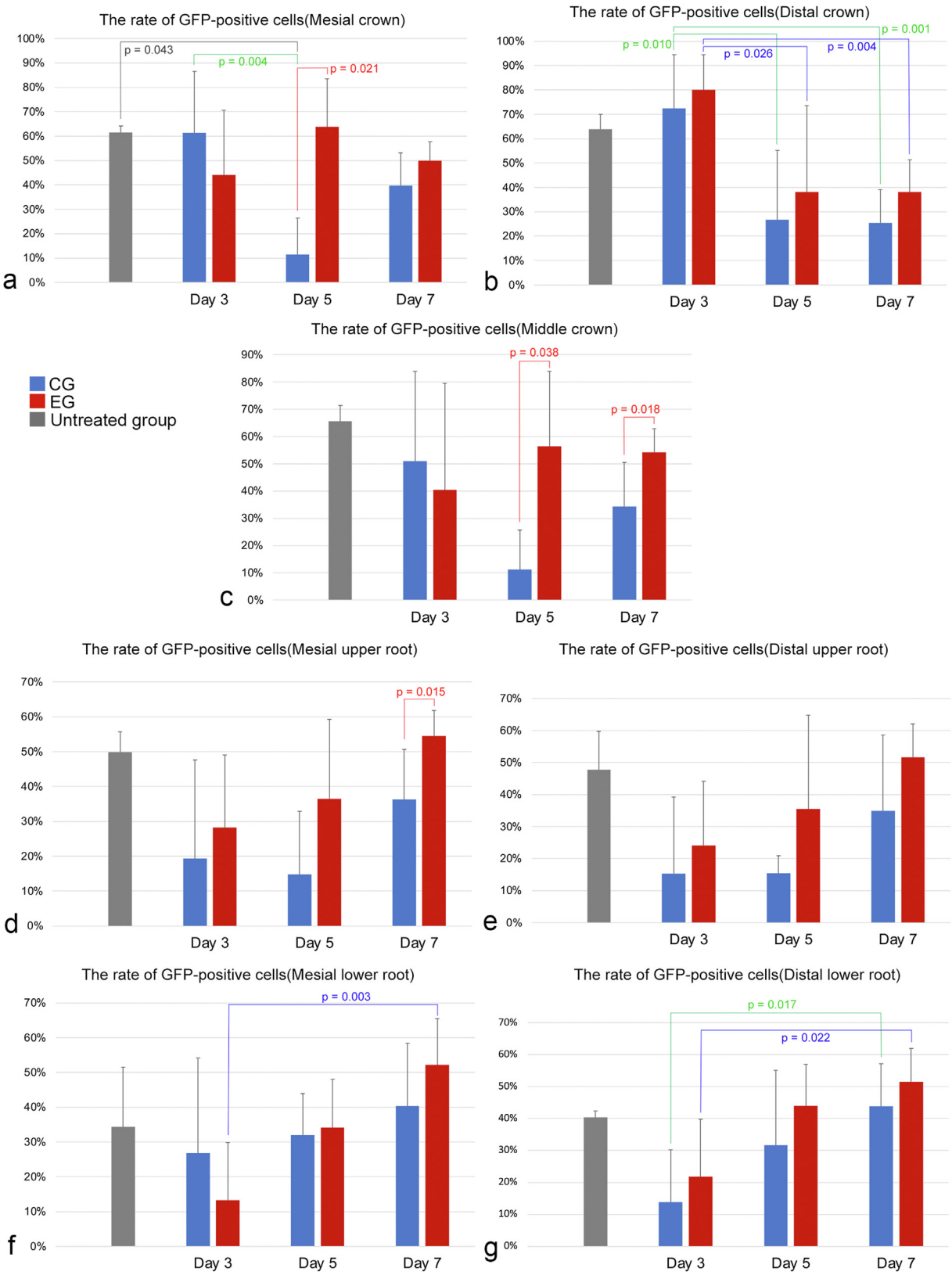

Fig. 5. The rates of green fluorescent protein (GFP)-positive cells in the mesial coronal (a), meddle coronal (b), distal coronal (c), mesial upper root (d), distal upper root (e), mesial lower root (f), and distal lower root pulps (g) during days 3–7. (a, c) The rate of GFP-positive cells in the experimental group (EG) tends to be lower than that of the control group (CG) in the mesial and middle coronal pulps at day 3, whereas the rate of GFP-positive cells in the EG is significantly higher than that of the CG at day 5 in the mesial coronal pulp and at days 5 and 7 in the middle coronal pulp. (b) In the distal coronal pulp, the rate of GFP-positive cells at days 5 and 7 is significantly lower than that at day 3 in both the CG and EG. (d–g) The rate of GFP-positive cells in the roots progressively increased over time in both the CG and EG, reaching the same or higher rate of GFP-positive cells as the untreated group on day 7 (d–g) The rate of GFP-positive cells in the EG tends to be higher than that in the CG. (d) The rate of GFP-positive cells in the mesial upper root in the EG is significantly higher than that of the CG at day 7. (f, g) In the lower roots, the rate of GFP-positive cells at day 7 significantly increases compared with that at day 3 in both the CG and EG except for the mesial lower root of the CG.

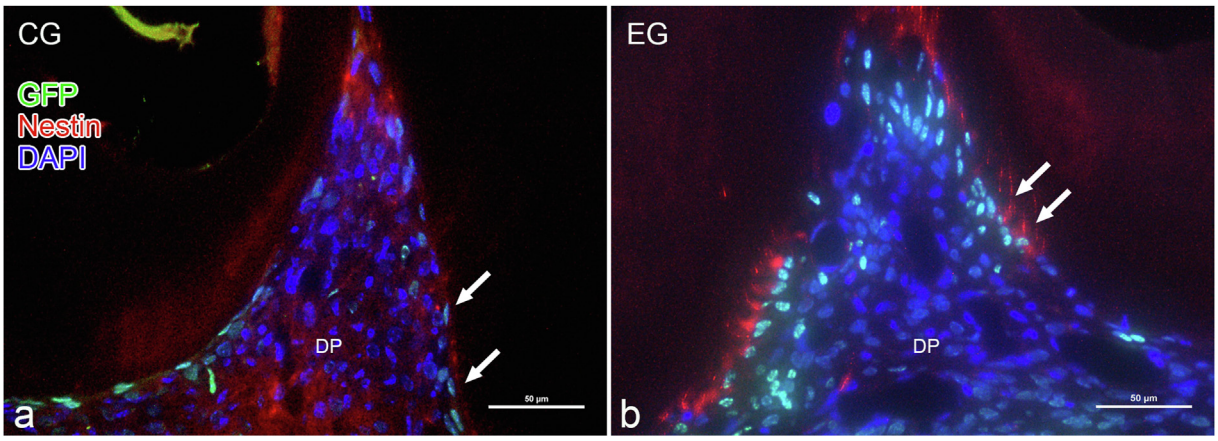

Fig. 6. Expression of green fluorescent protein (GFP) and Nestin in the pulp horns at day 7 after tooth replantation. Cell nuclei are counterstained with 4′,6-diamidino-2-phenylindole (DAPI). (a, b) GFP-positive cells (colored with green) that are aligned along the pulp–dentin border show Nestin-immunoreactivity (colored with red) at day 7 in both the CG and EG (arrows). DP, dental pulp. Scale bars = (a, b) 50 μm.

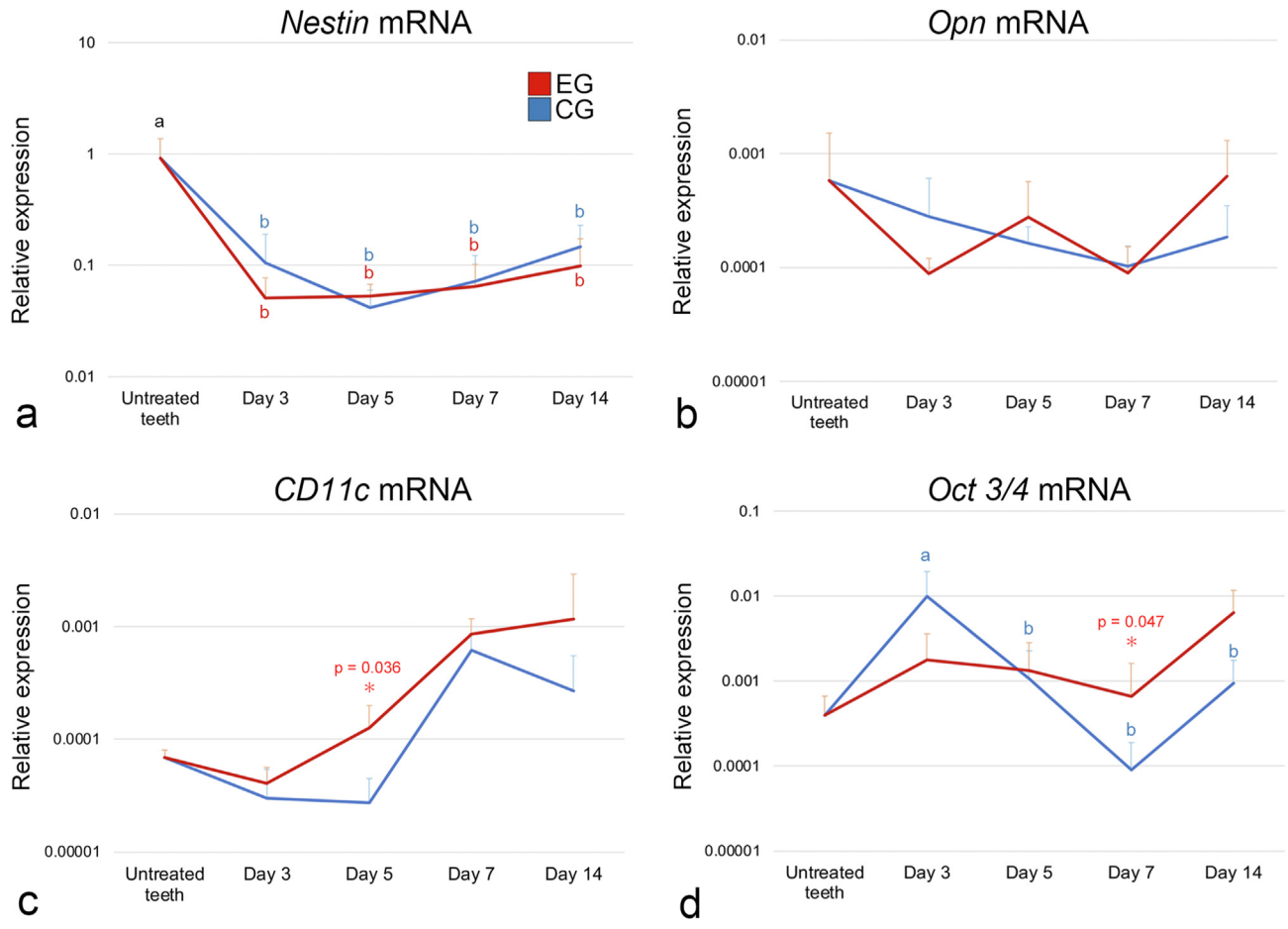

Fig. 7. mRNA expression of *Nestin* (a), *Opn* (b), *CD11c* (c), and *Oct3/4* (d) relative to *β-actin* mRNA expression. (a) *Nestin* mRNA in both the control group (CG) and experimental group (EG) is significantly decreased at days 3, 5, 7, and 14 compared with that of the untreated teeth ($p < 0.001$ between each group). (b) *Opn* mRNA expression in the EG tends to be lower than that in the CG at day 3 and to be higher than that of the CG at day 14. (c) *CD11c* mRNA decreases on the day 3 in both the CG and EG and increases at day 5 in the EG and at day 7 in the CG. *CD11c* mRNA in the EG at day 5 is significantly higher than that of the CG, and tends to be higher than that of the CG at day 14. (d) Although *Oct3/4* mRNA in the CG tends to be higher than that of the EG on day 3, the trend reverses at day 5, showing a higher expression of *Oct3/4* mRNA in the EG than that of the CG. At day 7, *Oct3/4* mRNA expression in the EG is significantly higher than in the CG. *Oct3/4* mRNA expression at days 5, 7, and 14 in the CG was significantly decreased compared with that at day 3 ($p = 0.041$, 0.013, and 0.022, respectively). Significant differences among the different stages are represented by different letters ($p < 0.05$).

the CG. *CD11c* mRNA in the EG at day 5 was significantly higher than of in the CG, and tended to be higher than that of the CG at day 14 (Fig. 7c). Although *Oct3*/4 mRNA in the CG tended to be higher than that of the EG at day 3, the trend reversed at day 5, showing a higher expression of *Oct3*/4 mRNA in the EG than that of the CG. At day 7, the *Oct3*/4 mRNA expression in the EG was significantly higher than that of the CG. *Oct3*/4 mRNA expression at days 5, 7, and 14 in the CG was significantly decreased compared with that at day 3 ($p = 0.041$, 0.013, and 0.022, respectively) (Fig. 7d).

4. Discussion

4.1. Effects of intentional perforation before tooth replantation on the dynamics of quiescent dental pulp stem cells and the pulpal healing process

In this study a new animal experimental model was developed that combines the intentional perforation of the pulp chamber floor before tooth replantation with GFP label chasing experiment using TetOP-H2B-GFP mice. It was demonstrated that the early revascularization into the pulp cavity after tooth replantation contributes to the survival and activation of quiescent DPSCs. Early revascularization occurred in the EG, and Nestin-positive perimeter tended to become higher than that of the CG at days 5 and 7 in both the mesial and distal pulps. The results obtained in this study using C57BL/6 mice were similar to those demonstrated in a previous study using ICR mice [5]. The rate of GFP-positive cells in the EG tended to be lower than that of the CG in the mesial and middle coronal pulps at day 3, and then tended to become higher than that of the CG at days 5 and 7. These findings suggest that quiescent DPSCs initially degenerated at day 3 due to the perforation at the pulp camber floor, but the early revascularization via the perforation site prevented the subsequent hypoxia-derived degeneration of the quiescent DPSCs in the coronal pulp and promoted OBLC differentiation. In the CG, revascularization begins from the root foramina, and the quiescent DPSCs may have been extensively degenerated due to hypoxia at day 5, because it takes time for revascularization into the coronal pulp. GFP-positive cells were aligned along the pulp–dentin border and showed Nestin-immunoreactivity at day 7 in both the CG and EG, supporting that quiescent DPSCs differentiated into OBLCs.

The rate of GFP-positive cells in the mesial and middle coronal pulps in the EG was significantly higher than that of the CG at days 5 and/or 7. However, there was no significant difference between the EG and CG at days 5 and 7 in the distal pulp. The bias in the perforated position toward the mesial root pulp may reduce the perforation effect on the healing process in the distal coronal pulp of the EG. The rate of GFP-positive cells in the mesial and distal upper root pulps in the EG tended to be higher than that of the CG during the observation period, and were significantly increased in the mesial upper root pulp at day 7. The rate of GFP-positive cells in the mesial and distal lower root pulps in the EG tended to be higher than that of the CG, although the difference between the two groups was smaller compared with that of the upper root pulps. These findings suggest that revascularization via the perforation site occurred in the EG, resulting in the early revascularization of the upper root pulps and the migration of the proliferating survived quiescent DPSCs in the coronal pulp to the upper root pulps.

4.2. Dynamics of pulpal healing-related factors after tooth replantation

In the quantitative RT-PCR analysis of the pulpal healing-related factors, *Nestin* mRNA in both the CG and EG showed similar expression levels but was significantly decreased at days 3, 5, 7, and 14 compared with that of the untreated group. These results are inconsistent with the protein expression demonstrated by the Nestin-positive perimeter. This contradictory result may be attributed to the different analysis methods used. The Nestin mRNA was quantified for expression throughout the dental pulp, whereas the Nestin protein was qualitatively analyzed by focusing on the odontoblasts or OBLCs at the pulp–dentin border. CD11c is a transmembrane glycoprotein expressed on the cell surface of monocytes, macrophages, and dendritic cells. *CD11c* mRNA decreased at day 3 in both the CG and EG and increased at day 5 in the EG, and day 7 in the CG. *CD11c* mRNA in the EG at day 5 was significantly higher than that of the CG. The appearance of dendritic cells along the pulp–dentin border has been reported to precede the appearance of newly differentiating OBLCs [22]. Dendritic cells are considered to play a role in promoting the differentiation of OBLCs after tooth injury [9]. Perforating the pulp chamber floor before tooth replantation may facilitate dendritic cell migration because of the early revascularization, which results in the subsequent differentiation of quiescent DPSCs into OBLCs. Osteopontin (OPN) plays an important role in the differentiation and cellular activity of OBLCs after tooth injury [23], and immune cells including dendritic cells and differentiating odontoblast-lineage cells are the source of OPN [24]. Regarding the *Opn* mRNA expression, however, there was no significant difference between the EG and CG. Oct 3/4 is a transcription factor that plays a critical role in the maintenance of the stem cells' undifferentiated state. Although *Oct3*/4 mRNA levels in the CG tended to be higher than that of the EG at day 3, the trend subsequently reversed at day 5, and a higher *Oct3*/4 mRNA expression was observed in the EG compared with that of the CG, where *Oct3*/4 mRNA expression in the EG was significantly higher than that of the CG at day 7. These results suggest that tooth replantation activates the quiescent DPSCs and increases the *Oct3*/4 mRNA at day 3 in both groups, whereas quiescent DPSCs degenerated due to the delayed revascularization in the CG, resulting in significant decreases in *Oct3*/4 mRNA at days 5, 7, and 14.

5. Conclusions

This study revealed that the intentional perforation of the pulp chamber floor before tooth replantation promoted the survival of quiescent DPSCs in the coronal pulp and the putative migration of dendritic cells, which resulted in the improved pulpal healing compared with the immediate tooth replantation model. The experimental model combining the pulp floor perforation and the chase of label-retaining cells using TetOP-H2B-GFP mice is advantageous in tracking the dynamics (*i.e.,* survival and differentiation) of DPSCs after tooth replantation. Therefore, the use of this model is expected to clarify the crosstalk mechanism between immune cells, including macrophages and dendritic cells, and DPSCs related to pulpal healing after tooth replantation, as well as to investigate the differentiation process of DPSCs into OBLCs.

Declaration of competing interest

The authors declare no conflicts of interest related to this study.

Acknowledgments

The authors cordially thank Dr. H. Ida-Yonemochi, Ms. Y. Abe, and Ms. M. Kawachi for their technical assistance and animal care, and Enago (www.enago.jp) for the English language review. This work was supported by Grants-in-Aid for Scientific Research (C) (nos. 20K10224 and 23K09411 to KN–O) and Research (B) (no. 23H03078 to HO) from the Japan Society for the Promotion of Science, Japan.

Appendix A. Supplementary data

Supplementary data to this article can be found online at https://doi.org/10.1016/j.reth.2023.10.004.

References

[1] Trope M. Clinical management of the avulsed tooth: present strategies and future directions. Dent Traumatol 2002;18:1–11.
[2] Andersson L, Andreasen JO, Day P, Heithersay G, Trope M, Diangelis AJ, et al. International Association of Dental Traumatology guidelines for the management of traumatic dental injuries: 2. Avulsion of permanent teeth. Dent Traumatol 2012;28:88–96.
[3] Fouad AF, Abbott PV, Tsilingaridis G, Cohenca N, Lauridsen E, Bourguignon C, et al. International Association of Dental Traumatology guidelines for the management of traumatic dental injuries: 2. Avulsion of permanent teeth. Dent Traumatol 2020;36:331–42.
[4] Kling M, Cvek M, Mejare I. Rate and predictability of pulp revascularization in therapeutically reimplanted permanent incisors. Endod Dent Traumatol 1986;2:83–9.
[5] Sano H, Nakakura-Ohshima K, Okada Y, Sato T, Ohshima H. The effect of intentionally perforating the floor of the pulp chamber on pulpal healing after tooth replantation in mice. J Oral Biosci 2023;65:31–9.
[6] Shimizu A, Nakakura-Ohshima K, Noda T, Maeda T, Ohshima H. Responses of immunocompetent cells in the dental pulp to replantation during the regeneration process in rat molars. Cell Tissue Res 2000;302:221–33.
[7] Hasegawa T, Suzuki H, Yoshie H, Ohshima H. Influence of extended operation time and of occlusal force on determination of pulpal healing pattern in replanted mouse molars. Cell Tissue Res 2007;329:259–72.
[8] Saito K, Ohshima H. Differentiation capacity and maintenance of dental pulp stem/progenitor cells in the process of pulpal healing following tooth injuries. J Oral Biosci 2017;59:63–70.
[9] Quispe-Salcedo A, Ohshima H. The role of dendritic cells during physiological and pathological dentinogenesis. J Clin Med 2021:10.
[10] Li L, Clevers H. Coexistence of quiescent and active adult stem cells in mammals. Science 2010;327:542–5.
[11] Honda M, Ohshima H. Biological characteristics of dental pulp stem cells and their potential use in regenerative medicine. J Oral Biosci 2022;64:26–36.
[12] Imai C, Sano H, Quispe-Salcedo A, Saito K, Nakatomi M, Ida-Yonemochi H, et al. Exploration of the role of the subodontoblastic layer in odontoblast-like cell differentiation after tooth drilling using Nestin-enhanced green fluorescent protein transgenic mice. J Oral Biosci 2022;64:77–84.
[13] Sonoyama W, Liu Y, Fang D, Yamaza T, Seo BM, Zhang C, et al. Mesenchymal stem cell-mediated functional tooth regeneration in swine. PLoS One 2006;1:e79.
[14] Wongwatanasanti N, Jantarat J, Sritanaudomchai H, Hargreaves KM. Effect of bioceramic materials on proliferation and odontoblast differentiation of human stem cells from the apical papilla. J Endod 2018;44:1270–5.
[15] Ishikawa Y, Ida-Yonemochi H, Suzuki H, Nakakura-Ohshima K, Jung HS, Honda MJ, et al. Mapping of BrdU label-retaining dental pulp cells in growing teeth and their regenerative capacity after injuries. Histochem Cell Biol 2010;134:227–41.
[16] Nakakura-Ohshima K, Quispe-Salcedo A, Sano H, Hayasaki H, Ohshima H. The effects of reducing the root length by apicoectomy on dental pulp revascularization following tooth replantation in mice. Dent Traumatol 2021;37:677–90.
[17] Plakwicz P, Cudziło D, Czochrowska EM, Gawron K, Kuc-Michalska M, Kukuła KT. Pulp revascularization after autotransplantation of the mandibular canines with partially resected roots: report of 5 cases with follow-ups between 26 and 80 months. J Endod 2023;49:478–86.
[18] Saito K, Ohshima H. The putative role of insulin-like growth factor (IGF)-binding protein 5 independent of IGF in the maintenance of pulpal homeostasis in mice. Regen Ther 2019;11:217–24.
[19] Foudi A, Hochedlinger K, Van Buren D, Schindler JW, Jaenisch R, Carey V, et al. Analysis of histone 2B-GFP retention reveals slowly cycling hematopoietic stem cells. Nat Biotechnol 2009;27:84–90.
[20] Ishikawa Y, Ida-Yonemochi H, Saito K, Nakatomi M, Ohshima H. The Sonic hedgehog–Patched–Gli signaling pathway maintains dental epithelial and pulp stem/progenitor cells and regulates the function of odontoblasts. Front Dent Med 2021;2:651334.
[21] Kilkenny C, Browne WJ, Cuthill IC, Emerson M, Altman DG. Improving bioscience research reporting: the ARRIVE guidelines for reporting animal research. J Pharmacol Pharmacother 2010;1:94–9.
[22] Nakakura-Ohshima K, Watanabe J, Kenmotsu S, Ohshima H. Possible role of immunocompetent cells and the expression of heat shock protein-25 in the process of pulpal regeneration after tooth injury in rat molars. Microscopy 2003;52:581–91.
[23] Saito K, Nakatomi M, Ida-Yonemochi H, Ohshima H. Osteopontin is essential for type I collagen secretion in reparative dentin. J Dent Res 2016;95:1034–41.
[24] Saito K, Nakatomi M, Ida-Yonemochi H, Kenmotsu S, Ohshima H. The expression of GM-CSF and osteopontin in immunocompetent cells precedes the odontoblast differentiation following allogenic tooth transplantation in mice. J Histchem Cytochem 2011;59:518–29.